Linear mountain waves past a mountain range with concavity and convexity

Kazuo Saito[1,2,3]

[1]Atmosphere and Ocean Research Institute/University of Tokyo, [2]Meteorological Research Institute, [3]Japan Meteorological Business Support Center

1. 3-D linear mountain waves (Smith 1980)

Governing #-D linear equations

$$U\frac{\partial u'}{\partial x}+\frac{1}{\rho_0}\frac{\partial p'}{\partial x}=0 \qquad (1-x)$$

$$U\frac{\partial v'}{\partial x}+\frac{1}{\rho_0}\frac{\partial p'}{\partial y}=0 \qquad (1-y)$$

$$\sigma U\frac{\partial w'}{\partial x}+\frac{1}{\rho_0}\frac{\partial p'}{\partial z}=b' \qquad (2'')$$

$$\frac{\partial u'}{\partial x}+\frac{\partial v'}{\partial y}+\frac{\partial w'}{\partial z}=0 \qquad (3'')$$

$$U\frac{\partial b'}{\partial x}+w' N^2=0 \qquad (4'')$$

Eliminating *u'* and v' from *(1-x),(1-y),(3")*

$$(U\frac{\partial^2 w\prime}{\partial x\partial z}-\frac{1}{\rho_0}(\frac{\partial^2 p\prime}{\partial x^2}+\frac{\partial^2 p\prime}{\partial x^2})=0 \qquad (5')$$

Eliminating p' *in* conjunction with (2") and (4") yields

$$\frac{\partial^2}{\partial x^2}\{\sigma\left(\frac{\partial^2 w'}{\partial x^2}+\frac{\partial^2 w'}{\partial y^2}\right)+\frac{\partial^2 w'}{\partial z^2}\}+\frac{N^2}{U^2}(\frac{\partial^2 w\prime}{\partial x^2}+\frac{\partial^2 w\prime}{\partial y^2})=0 \qquad (6')$$

Here, σ is the parameter for hydrostatic approximation; σ=0 for hydrostatic and σ=1 for nonhydrostatic

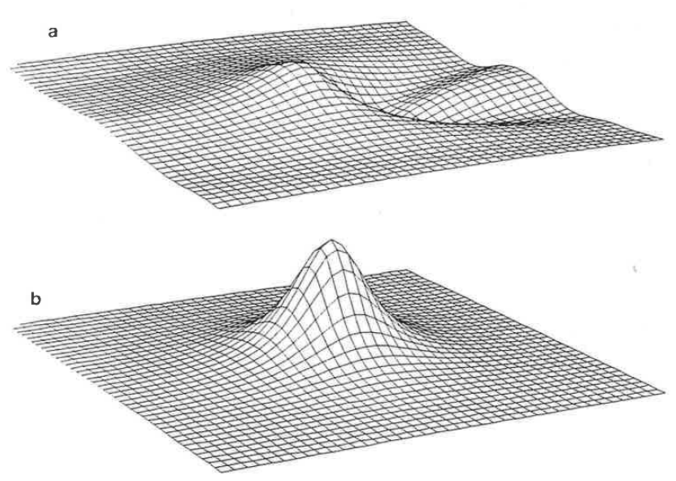

The statics solution with a large horizontal scale mountain shows a boomerang-shaped upwelling above the mountain

Smith (1989)

2. Investigation of "Karakkaze" by Nishi, Kusaka, et al.

Statistical analysis and numerical experiments on the characteristics of the winter monsoon "gusts" in the Kanto region over terrain that is convex on the upwind side (concave on the downwind side).

(a) 2002/02/19 1200 LST

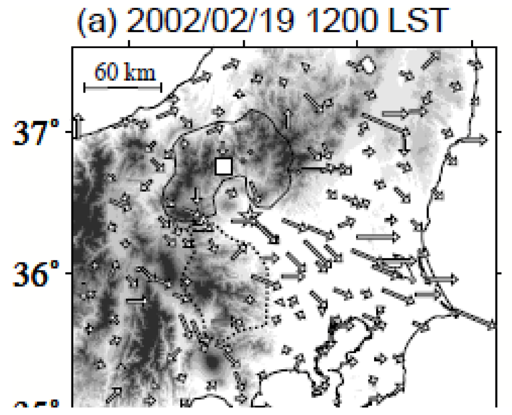

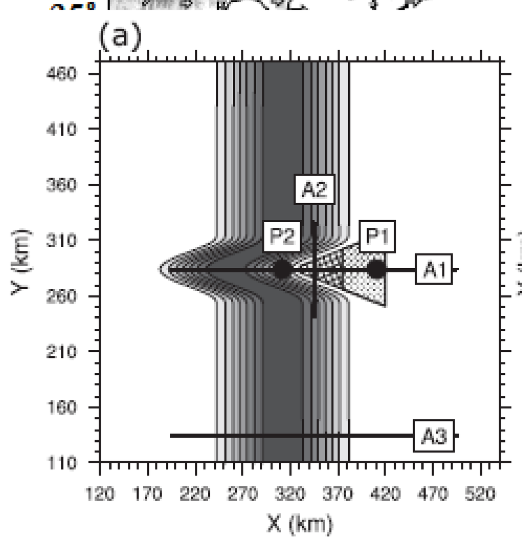

$$MNT(x,y)=\begin{cases}\frac{H}{2}\left(1-\cos\left(\frac{2\pi(x-a)}{L_W}\right)\right) & a\le x\le a+L_W;\\ 0 & \text{otherwise.}\end{cases}$$

where

$$a=\begin{cases}X_c-\frac{L_W}{2}-A_b\sin\left(\frac{\pi}{L_b}(y+L_b-Y_c)\right)^2, & Y_c-\frac{L_b}{2}\le y\le Y_c+\frac{L_b}{2};\\ X_c-\frac{L_W}{2}, & \text{otherwise.}\end{cases}$$

3. Computation of linear analytic solution

The nature of airflow over a terrain convex on the windward side (concave on the leeward side), as treated by Nishi and Kusaka et al. is discussed using a 3-D mountain waveform analysis solution.

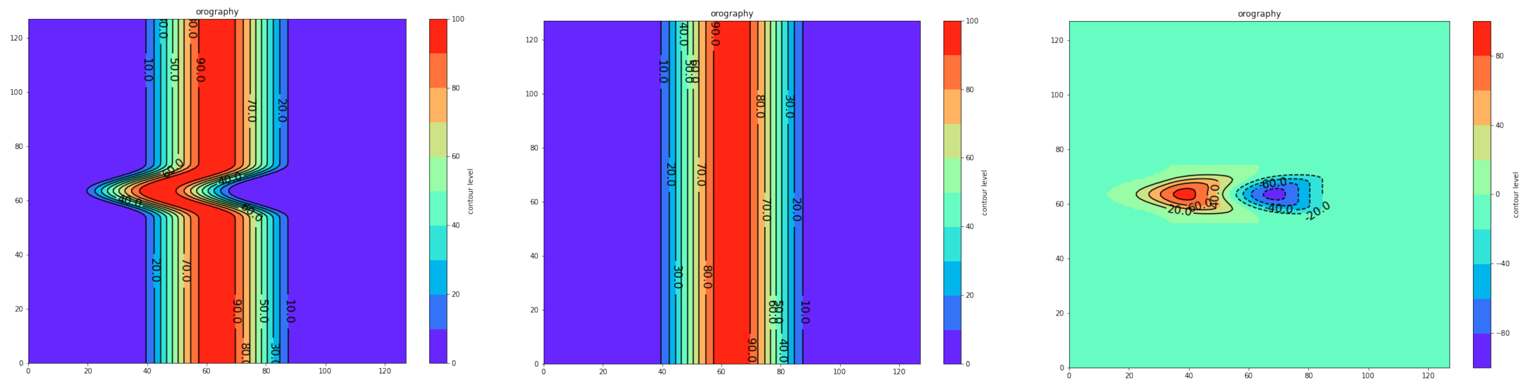

Topography is convex on the windward side (concave on the leeward side)

Bell cosine mountain range terrain

Difference between the two

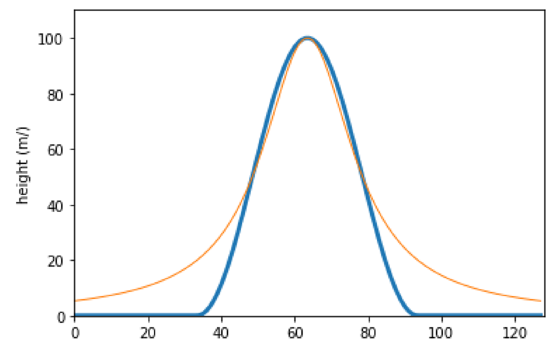

Bell-shaped (switch of Agnesi) mountain

$$h(x)=\frac{h_m}{1+(\frac{x-x_c}{a})^2}$$

Mountains of Belko signs

$$h(x)=\frac{h_m}{2}\{1-\cos(2\pi(x-x_c)/a)\}$$

For vertical displacement δ

$$\frac{\partial^2}{\partial x^2}\{\sigma\left(\frac{\partial^2}{\partial x^2}+\frac{\partial^2}{\partial y^2}\right)+\frac{\partial^2}{\partial z^2}\}\delta+\frac{N^2}{U^2}(\frac{\partial^2}{\partial x^2}+\frac{\partial^2}{\partial y^2})\delta=0 \qquad (5'')$$

The following formula is used to calculate the solution of (5'')

$$\delta(x,\ y,\ z)=\iint_{-\infty}^{\infty}H(k,\ l)e^{imz}e^{i(kx+ly)}dkdl,$$

The Fourier transform was performed on a horizontal 128*128 grid, and a horizontal grid spacing of 3 km was assumed. In the vertical direction, 32 layers were taken at 400 m. General wind *U* = 10 m/s and atmospheric stability *N* = 0.01/s were assumed.

4. Results

1) Case of concavity in the lee side and convexity in the windward side

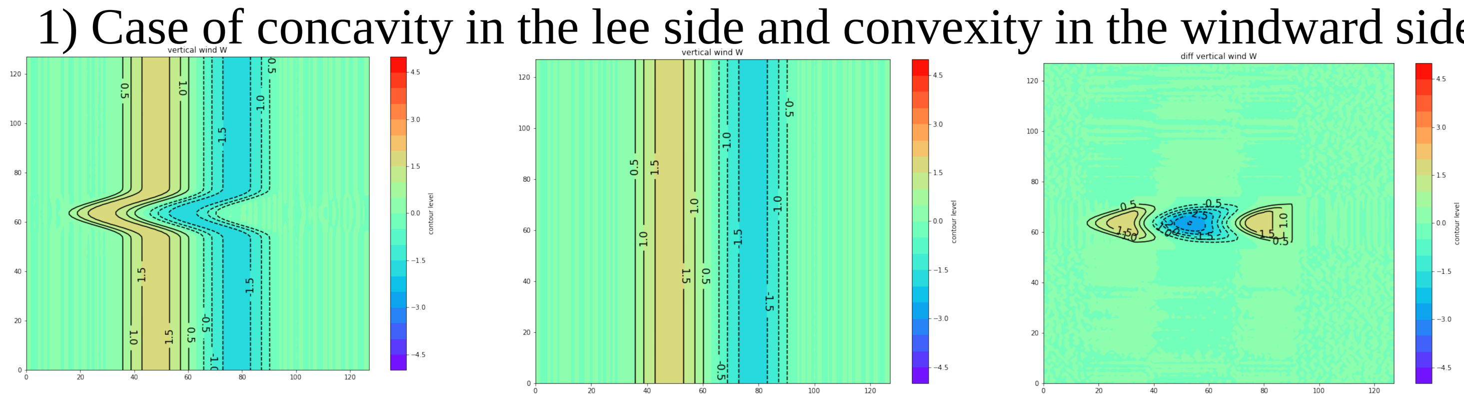

Vertical motion at surface for convex topography, bell-cosine mountain range and the difference.

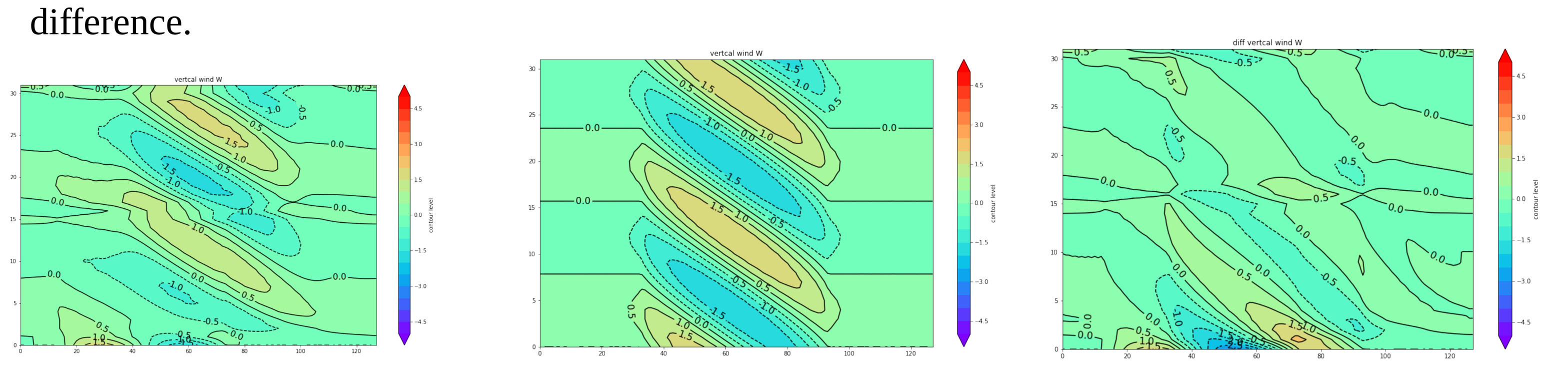

Horizontal wind cross-section

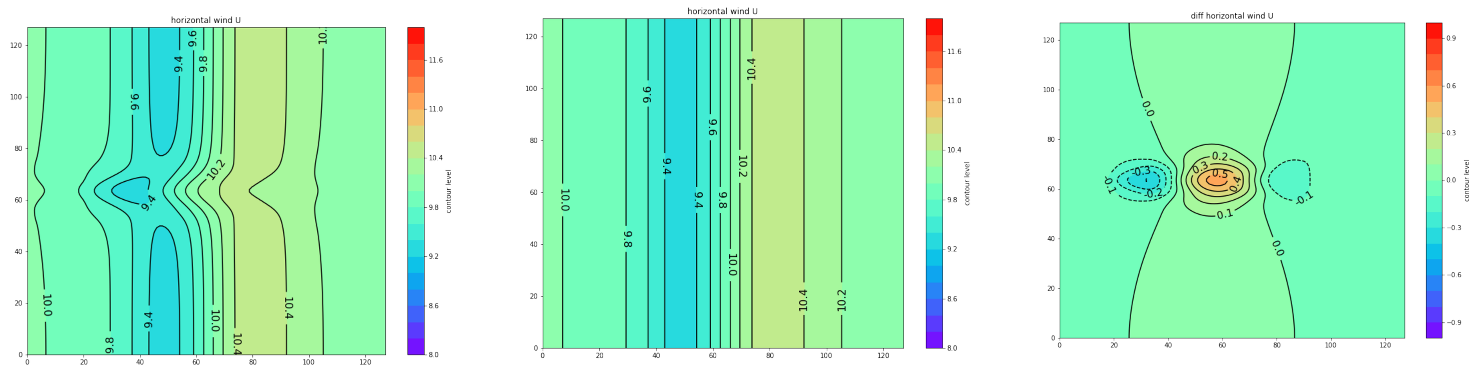

Surface horizontal wind

2) Case of concavity in the lee side

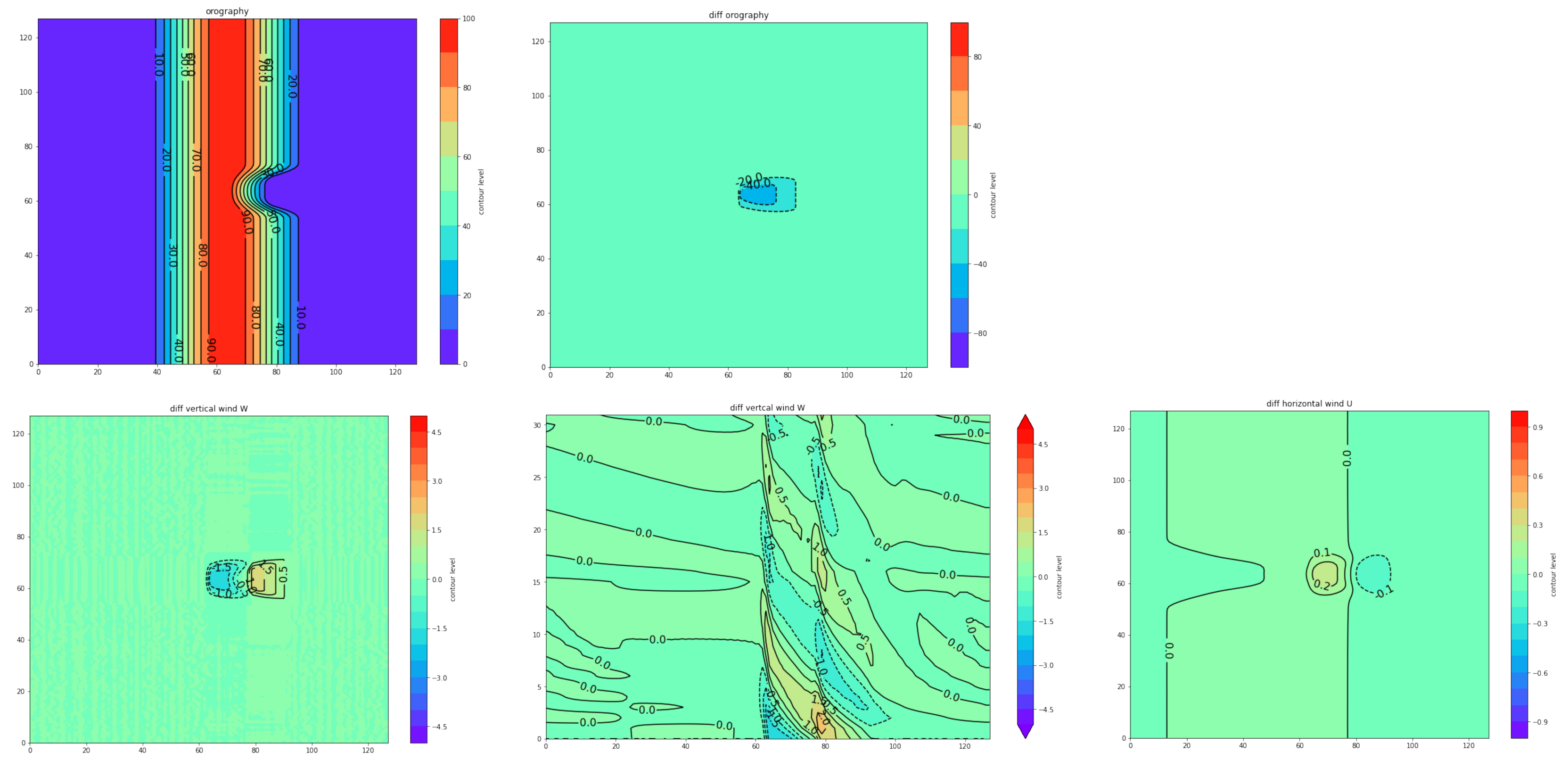

Vertical motion at surface, horizontal wind cross-section and at surface

3) Case of convexity in the windward side

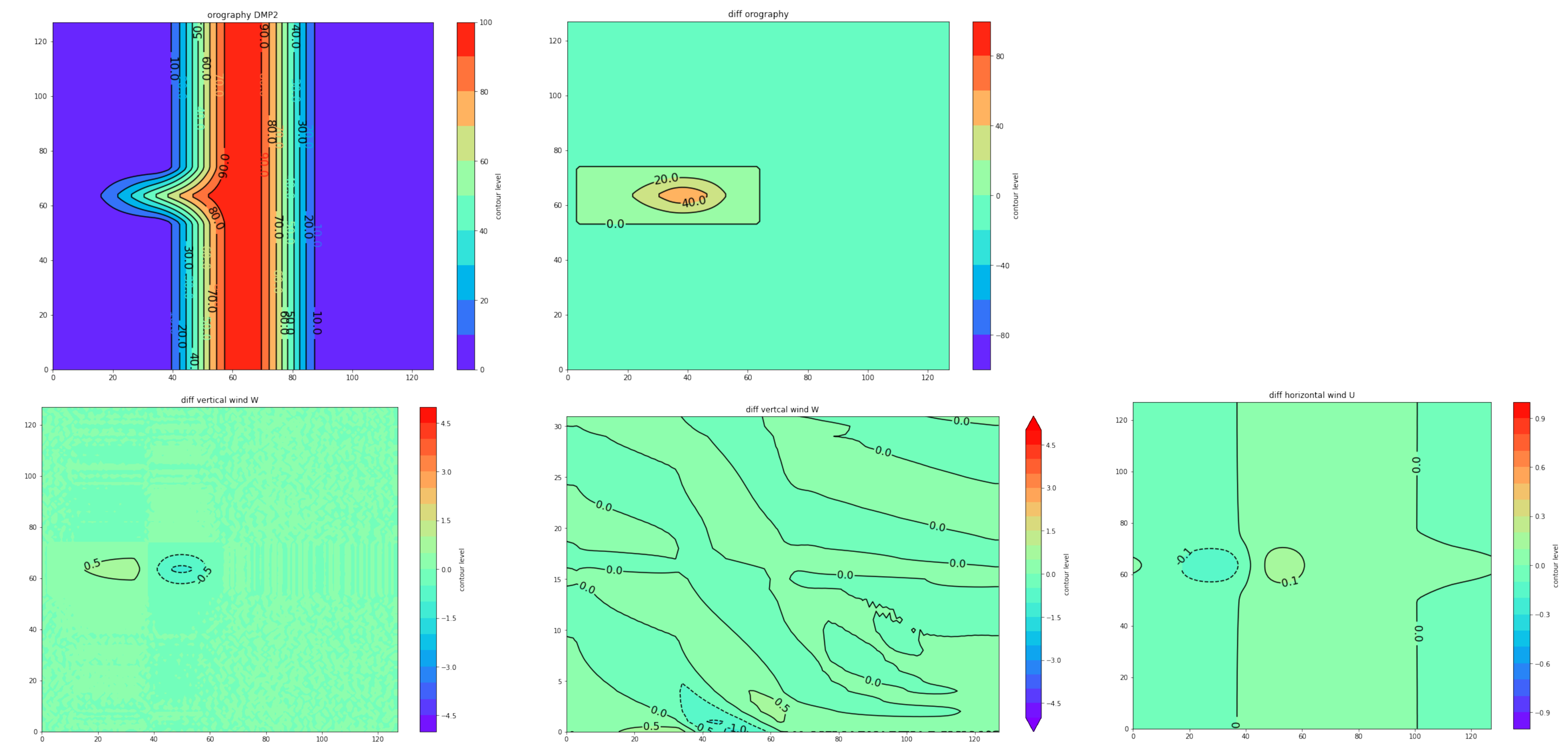

Vertical motion at surface, horizontal wind cross-section and at surface

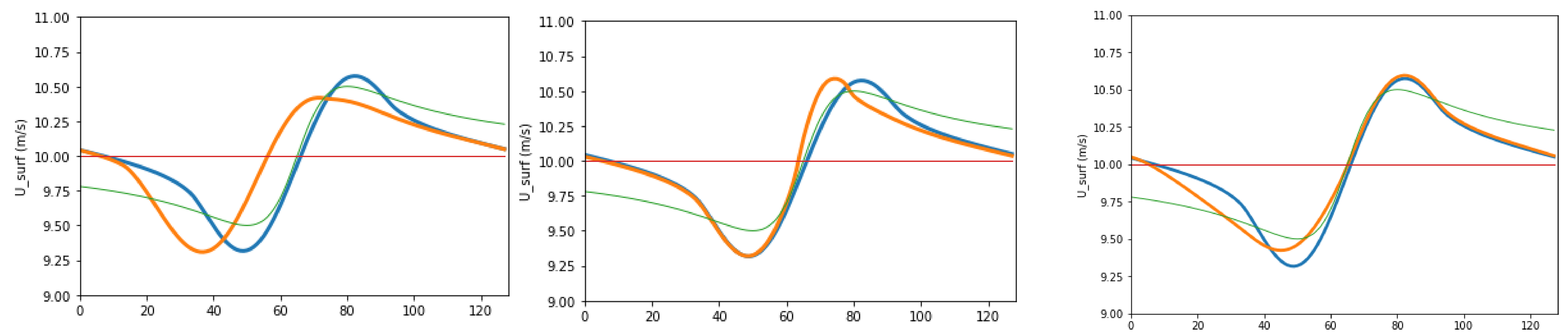

Surface horizontal wind seed. Witch of Agnessi, Cosine bell, fore case (1), (2), and (3)

5. Summary

In the case of the folded terrain of Nishi and Kusaka (2019), surface winds are greater in the concave downwind side than in the concave, but do not exceed those of the 2D terrain in terms of grated wind intensity.

When the peak was cut into a concave shape on the downwind side without changing the position of the axis of the peak, the maximum wind magnitude was greater than that of the 2D terrain. This may be due to the effect of the asymmetric topography with steeper slope on the downwind side than on the upwind side.

When convex topography was added to the windward side, the blocking moved to the windward side and the maximum wind was slightly greater. This may be due to the effect of asymmetric topography with a slower slope on the upwind side.

References:

Nishi, A. and H. Kusaka, 2019: J. Meteor. Soc. Japan, 97, 787-803.

Saito, K., G. Doms, U. Schaetter and J. Steppeler, 1998: 3-D mountain waves by the Lokal-Modell of DWD and the MRI-mesoscale nonhydrostatic model. Pap. Meteor. Geophys., 49, 7-19.

Smith, R. B., 1980: Linear theory of stratified hydrostatic flow past an isolated mountain. Tellus, 32, 348-364.